International Journal of u- and e- Service, Science and Technology
Vol.9, No. 11 (2016), pp.217-226
http://dx.doi.org/10.14257/ijunesst.2016.9.11.19

The Swing Angle of Insulators Measurement Based on Binocular Vision and Improved Region Segmentation

Rongbao Chen[1,a], Yang Li[1,b], Dongbo Weng[2] and Tianze Fei[1]

[1]*School of Electrical Engineering and Automation, Hefei University of Technology, Hefei, China*
[2]*Huainan Power Supply Company, State Grid, Huainan, China*
[a]*crbwish@126.com*,[b]*lyhfut09@163.com*

Abstract

This paper first analyzed the structure and the edge symmetry of insulator and divided the insulator into 8 kinds of edge according to these characteristics. Then it improved the algorithms that segment and label the region of interest (ROI) based on the depressed region of insulator, which makes labeling multi-insulators in a single image solved. To accurately extract the edge of insulator from the ROI, this paper proposed the double thresholds edge detecting method on account of parallax principle in binocular vision, avoiding of the deficiency of under-filtering and over-filtering within the single threshold method based on monocular vision. It analyzed and removed local and global irrelevant pixels using statistical methods, thereby stereoscopically matched the pixels in each ROI and calculated their 3D coordinates. Then 2 vectors are constructed based on the maximum and minimum of the Z coordinate component: the vertical vector and the direction vector of the insulator. Finally, every swing angle can be calculated using the inner product method. Experiment results show that the relative error of this method is less than 1.3%, it not only has higher accuracy than the traditional method, but also avoids the low efficiency of a single swing angle measurement of traditional method.

Keywords*: binocular vision; ROI segmentation; double threshold edge detection; swing angle of insulators; OpenCV*

1. Introduction

The high-voltage transmission line inevitably crosses the complex environment, and makes maintenance with difficulty. The lines are usually hung on insulator, which is installed on transmission tower. Its poor lateral stability coupled with wind easily leads to windage yaw. This deflection usually causes trip breakdown. Scholars defined the angle between the current and initial vertical position of insulator as swing angle or windage yaw angle (We simply call it as angle below). The bigger angle shows that the deflection is more serious and the live end of bottom is closer to the transmission tower, when the distance between them is less than minimum air discharge gap, windage yaw discharge will occur, which causes the trip breakdown or even large area blackout accident [1-2].

Many scholars research on the angle measurement. Xinbo Huang, *etc.*, in paper [3] used the wireless detecting instrument, which calculates the angle according to upper and lower angles. Shengxue Wang, *etc.*, in paper [4] established rigid body model of insulator by means of rigid body statics and then calculated the angle using geometric method. Deyi Kong, *etc.*, in paper [5] used Analysis System (ANSYS) to establish the coupling model of transmission tower, insulator and wire. These methods depend on the ideal model and can't simulate all the natural environment of insulator. Haijun Lu, *etc.*, in paper [6] used image processing technique to detect the insulator and calculate the angle, but can only deal with image that contains a single insulator and difficult to isolate insulators from complex background.

ISSN: 2005-4246 IJUNESST

This paper proposed the label method and the angle measurement based on stereo vision technique. The process can be divided into three aspects: (1) Region of interest (ROI) segmenting and labeling; (2) Contour extracting; (3) Matching and calculating.

2. Improved ROIs Label Method

ROIs labeling is giving a unique number to each ROI. All pixels label in one region is same. The traditional labeling algorithm such as line scanning is very suitable for real-time computing because of its fast speed, but it scans just one time and returns large error. We proposed an improved labeling algorithm pointing at shape of insulator.

2.1. Edge Symmetry

2.2. Strength Analysis

Lienhart in paper [7] discussed the texture features of the edge and Clark in paper [8] researched the characteristic of symmetrical edge. They both elaborated on such a hypothesis: In some symmetric objects, the angle histogram of edge has rotational symmetry. This strength of symmetric is calculated as follows:

$$M = \frac{1}{E}\sum_{\varphi=0}^{\pi}\left(A(\varphi) - A(\varphi+\pi)\right)^2 \quad (1)$$

In Eq. (1), $A(\varphi)$ is the sum of edge amplitude in direction φ, E is a normalization factor. We can divide insulator into 8 kinds of edge according to its shape characteristics as shown in Figure 1. The point 'T' is the edge pixel, the black points is the pixel of insulator. The direction φ of each edge pixel is determined by its eight surrounding contiguous pixels.

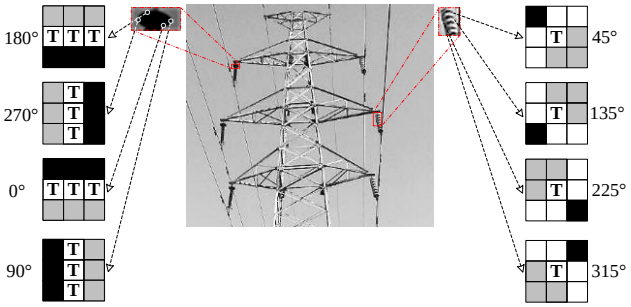

Figure 1. The Symmetric of Edge Pixels

The histogram of all edge points in the same region is calculated as follows:

$$HOE[\varphi] = Num(EP|_{\varphi}) \quad (2)$$

In Eq. (2), $\varphi \in \{0°, 45°, 90°, 135°, 180°, 225°, 270°, 315°\}$, $HOE[\varphi]$ is the number of all edge points of the direction φ. An example of the edge points of the insulator is shown in Figure 2.

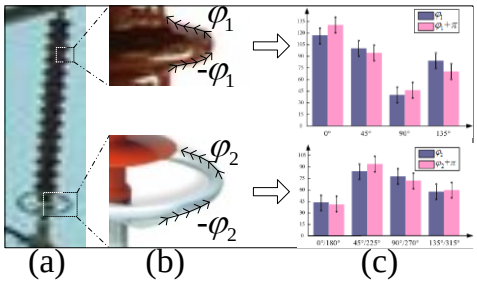

Figure 2. Edge Direction Histogram of Transition Region

It is clear that if there is an edge point of direction φ, there will be an edge point of the opposite direction to φ in a corresponding position by the step π along the edge of insulator. The edge histogram of insulator in Figure 2a, is shown in Figure 2c, which basically accords with the symmetry of the edge direction.

2.3. Improved Edge Tracking Algorithm

When a scan line is scanning a region, there are two intersections with boundary of insulator and the scan line: entry point and exit point. These two points constitute an interval. Especially, there are 2*n* intersections with boundary of sunken part in insulator and the scan line: *n* entry points and *n* exit points, which form *n* intervals. All pixels in these intervals belong to the same insulator. We can obtain a pixel sequence by means of edge tracking algorithm and the contour lines made of this sequence contain the insulator completely. It is easy to label ROIs by matching pixels with the sequence and forming the interval [9]. Then, we analyze how to match these pixels as shown in Figure 3.

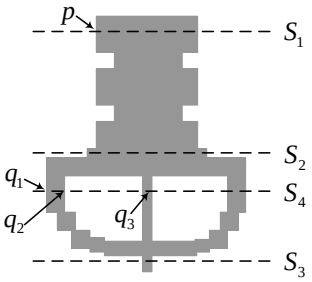

Figure 3. Scanning the Insulator

The algorithm just runs one time and stores these pixels in an array by row-coordinate when the scan lines S_1 and S_2 only intersect the insulator at p, then sorts column coordinates of the array rows in ascending order. After this, a labeled interval has been structured. For example, the algorithm will sort as [p_1, p_2, p_3, p_4] when there are 4 edge points in one row. Where, [p_1, p_2] and [p_3, p_4] form 2 intervals, respectively. Then the algorithm labels ROIs by these intervals. However, this method has 2 special cases:

1) The intersection is the entry point and the exit point simultaneously when there is only one pixel scanned by S_3 in the region.

2) S_4 has multiple intersections at entry and exit. The left and right pixels of some intersections such as q_3 both belong to an insulator and they are not the entry point and the exit point. The intersection can be the real entry or exit point only if one of the left and right pixels of this intersection is insulator and another is not (like q_1 and q_2).

In summary, this paper improved region segmenting and labeling algorithm, which brings into the strength of symmetric *M* and processes different types from left to right

and top to bottom. This improved algorithm can reduce the rate of error extraction. It is asymmetrical a little when $M < \lambda$ (λ is the threshold), which means it is a suspected ROI. The binary image array is *A*[*M*, *N*], the improved algorithm steps as follows:

1) Given the threshold λ ;

2) Initializing the label counter as *iLabel*=1 and setting the interval *pLabel*[*M*, *N*]. We stipulate *pLabel*[*i* ,0] as the number of edge pixels in the *i*-th row;

3) Finding the first edge pixel in the non-labeled region, the algorithm turns to step *6)* and ends up if this image has been searched, otherwise sets all elements in *pLabel*[*M*, *N*] to 0. Assigning the edge pixels the value *iLabel* and storing the column coordinates of the pixels in *pLabel*[*M*, *N*] when tracking edge of the region. After this, the algorithm gets the number of all edge pixels on each scan line in insulator and the starting line *sRow* and end line *eRow*;

4) Processing elements from *sRow* to *eRow* as follows:

(a) Staying the pixel if the left or right pixel of a edge pixel belongs to the insulator and another background or labeled region, otherwise deleting it from *pLabel*[*M*, *N*];

(b) Sorting column coordinates of the array rows in ascending order;

(c) Getting two elements in succession as the left and right endpoints of label sections. Labeling the pixels within the same segment one by one and judging whether the pixel belongs to the ROI before: “Yes" to label and "No" for having met the hollow region of insulator, then detecting the edge of the hollow region and assigning edge pixels the value *iLabel* storing the column coordinates of the pixels in *pLabel*[*M*, *N*]. After this, processing from the smallest row in hollow region until to *eRow* by step *a)*.

5) Calculating *M* of the current region and determining: saving the current label if $M < \lambda$, signing the corresponding ROI and *iLabel*=*iLabel*+1, otherwise *iLabel*=*iLabel*. After that, turning to the step *3)*.

6) Returning the value *iLabel* which is the number of insulator regions.

Process result is shown in Figure 4.

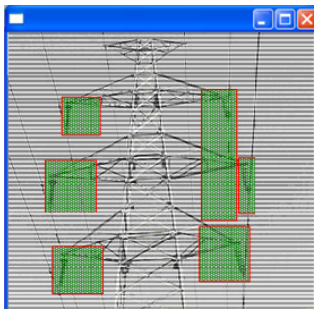

Figure 4. Segmented ROIs

3. Object Detecting based on Binocular Vision

In order to extract precise edge from ROI and reduce the influence from insulator’s internal structure, this paper proposed double thresholds edge detecting method based on binocular vision to, which well avoided insufficient extraction or excess extraction by single threshold method based on monocular vision, and removed irrelevant pixels with statistical method.

3.1. Double Threshold Detection Method based on Binocular Vision

The binocular vision consisting of 2 cameras obtains 2 photos of transmission tower at the same time. The left part of Figure 5, shows a binocular imaging principle diagram. The distance between the 2 optical centers of cameras is known as the baseline distance *B*,

and the camera focal length is f [10]. The vertical view is shown as the right part of Figure 5.

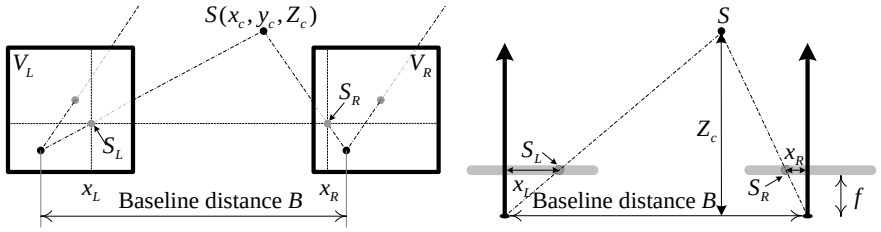

Figure 5. Binocular Vision Principle

This brings the pixel (x_L, y) in the left image V_L and (x_R, y) in V_R originating from a common scanline. Given 2 modifying factors, each new pair of captured images are hypothesized to be of background alone, and a image difference map (D) is calculated by block matching [11], based on the stored correspondences.

$$D(x_L, x_R, y) = \sum_{u,v} |V_L(x_L + u, y + v) - V_R(x_R + u, y + v)| \tag{3}$$

Let D represent a difference image for either left or right image, as obtained from Eq. (3). A simple [−1 1] edge operator is applied to D to generate an edge image, E. Clearly, positive edges are obtained on the left of a contour ridge in D and negative edges on the right. Disparity contours can be extracted by finding edge pairs, e^+ to the left of e^-, on the same scanline, satisfying the following conditions:

$$\begin{aligned} &1. E(e^+)/\max(E) > \tau_E, E(e^-)/\min(E) > \tau_E \\ &2. \left|E(e^+) + E(e^-)\right| < \varepsilon_E \\ &3. \forall_{p \in [e^+, e^-]} D(p) \geq \min(D(e^+), D(e^-)) \end{aligned} \tag{4}$$

In Eq. (4), Condition 1 excludes edge pixels below a threshold τ_E; Condition 2 requires that e^+ and e^- have similar edge response; condition 3 checks that line segment [e^+, e^-]corresponds to a high intensity edge ridge in D. The segments c= [e^+, e^-] are the desired edges, and their lengths $|c|$= $\boldsymbol{d}(c)$, the differential disparity between foreground and background from Eq. (5).

$$\boldsymbol{d}(c) = x_L(c^-) - x_L(c^+) \tag{5}$$

c^+ and c^- are left and right end pixels. Edge regions R can be formed by connecting edge line segments vertically. Unfortunately, this edge extractor is sensitive to the threshold τ_E. The higher the threshold, the more unwanted region is removed, but the more useful edges are lost.

a. b. c.

Figure 6. Threshold Segmenting Results

This paper proposed a double thresholds edge detecting method. Let the views $C_{\downarrow}$ Figure 6a, and $C^{\uparrow}$ Figure 6b, be the set of edge regions filtered by smaller threshold τ_E=$\tau_{\downarrow}$

and bigger threshold $\tau^{\uparrow}$, respectively. A new edge image C_* is generated by Eq. (6) as shown in Figure 6c. In our research, $\tau_{\downarrow}$=0.015 and $\tau^{\uparrow}$=0.05.

$$C_* = \left\{ R_{\downarrow} \in C_{\downarrow} \mid \exists R^{\uparrow} \in C^{\uparrow}, R_{\downarrow} \cap R^{\uparrow} = 0 \right\} \tag{6}$$

3.2. Removal Irrelevant Points based on the Statistical Analysis

As shown in Figure 6c, double thresholds method is used to keep the edge of insulator and reduce the unwanted region, but the effect is still not good. We statistically regularize the line segments and suppress edge region irrelevant pixels to remove remaining noise in C_*.

1) Firstly, eliminating the irrelevant pixels within insulator. Let R be an edge region containing $|R|$ line segments, $c \in R$ a line segment consisting of $|c|$ pixels, and $p \in c$ a pixel on c. The average intensity of c is:

$$\bar{\mathrm{i}}(c) = |c|^{-1} \sum_{p \in c} D(p) \tag{7}$$

Assume now that the average intensity $\bar{i}(c)$ and differential disparity $\boldsymbol{d}(c)$ are independent, and their distribution within R a bivariate Gaussian:

$$\eta\left(\bar{\mathrm{i}}(c), \boldsymbol{d}(c); \bar{\mathrm{i}}(R), \tilde{\boldsymbol{d}}(R); \sigma_{\mathrm{i}}(R), \sigma_{\boldsymbol{d}}(R)\right) \propto \frac{1}{\sigma_{\mathrm{i}}(R), \sigma_{\boldsymbol{d}}(R)} \exp\left[-\frac{\left(\bar{\mathrm{i}}(c) - \bar{\mathrm{i}}(R)\right)^2}{2\sigma_{\mathrm{i}}(R)^2} - \frac{\left(\boldsymbol{d}(c) - \tilde{\boldsymbol{d}}(R)\right)^2}{2\sigma_{\boldsymbol{d}}(R)^2} \right] \tag{8}$$

The mean values $\bar{\mathrm{i}}(R)$ and $\tilde{\boldsymbol{d}}(R)$ are

$$\bar{\mathrm{i}}(R) = \frac{\sum_{c \in R} \bar{\mathrm{i}}(c)}{|R|} \tag{9}$$

$$\tilde{\boldsymbol{d}}(R) = \frac{\sum_{c \in R} \bar{\mathrm{i}}(c) \boldsymbol{d}(c)}{\sum_{c \in R} \bar{\mathrm{i}}(c)} \tag{10}$$

Where $\tilde{\boldsymbol{d}}(R)$ is an average disparity weighted towards line segments with high $\bar{i}(c)$.

Deviations $\sigma_{\mathrm{i}}(R)$ and $\sigma_{\boldsymbol{d}}(R)$ are:

$$\sigma_{\mathrm{i}}(R) = \sqrt{|R|^{-1} \sum_{c \in R} \left(\bar{\mathrm{i}}(c) - \bar{\mathrm{i}}(R)\right)^2} \tag{11}$$

$$\sigma_{\boldsymbol{d}}(R) = \sqrt{|R|^{-1} \sum_{c \in R} \left(\boldsymbol{d}(c) - \tilde{\boldsymbol{d}}(R)\right)^2} \tag{12}$$

Define an integrated intensity/disparity measure and a coupled deviation:

$$\boldsymbol{\mu}_1(c, R) = \left|\bar{\mathrm{i}}(c) - \bar{\mathrm{i}}(R)\right| \left|\boldsymbol{d}(c) - \tilde{\boldsymbol{d}}(R)\right| \tag{13}$$

$$\tilde{\sigma}(R) = \sigma_{\mathrm{i}}(R) \sigma_{\boldsymbol{d}}(R) \tag{14}$$

We consider c an irrelevant pixel and remove it from its region R if

$$\boldsymbol{\mu}_1(c, R) > 2\tilde{\sigma}(R) \tag{15}$$

The above calculation eliminates most of the irrelevant pixels as shown in Figure 7.

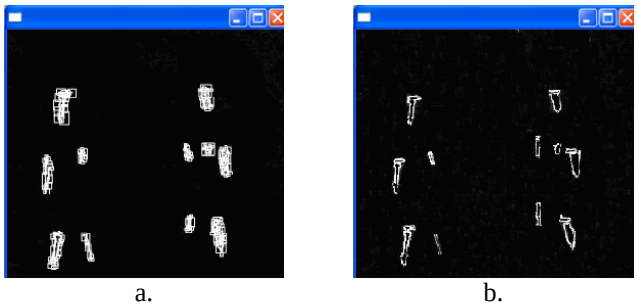

a. b.

Figure 7. Eliminating the Irrelevant Pixels within Insulators

2) Secondly, removing region irrelevant pixels globally. Let L be the set of $|L|$ edge regions just regularized. Since unwanted ROI is usually small and of low intensity, a summed intensity combining both attributes is calculated as follows:

$$\hat{\mathrm{i}}(R) = \bar{\mathrm{i}}(R)|R| \tag{16}$$

Another Gaussian distribution models the regions L in relative to the region with the largest summed intensity, R^*:

$$\eta\left(\hat{\mathrm{i}}(R), \hat{\mathrm{i}}(R^*), \hat{\sigma}(L)\right) \propto \frac{1}{\hat{\sigma}(L)} \exp\left[-\frac{\left(\hat{\mathrm{i}}(R) - \hat{\mathrm{i}}(R^*)\right)^2}{2\hat{\sigma}(L)^2}\right] \tag{17}$$

Where the deviation is:

$$\hat{\sigma}(L) = \sqrt{|L|^{-1} \sum_{R \in S} \left(\hat{\mathrm{i}}(R) - \hat{\mathrm{i}}(R^*)\right)^2} \tag{18}$$

An adaptive threshold removes irrelevant pixels globally from the set L:

$$\left|\hat{\mathrm{i}}(R) - \hat{\mathrm{i}}(R^*)\right| > \hat{\sigma}(L) \tag{19}$$

After iterative calculating, the global independent pixels are eliminated and the edge of insulator is obtained as shown in Figure 8a. Apply the edge after removal of local and global independent pixels to the original, as shown in Figure 8b.

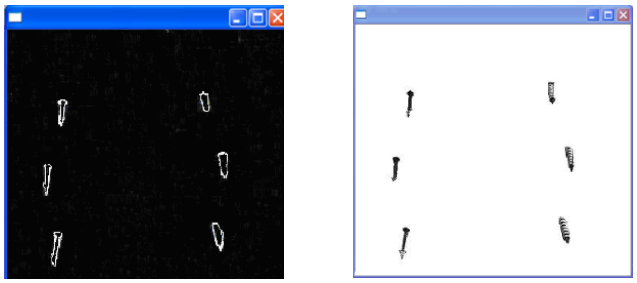

a. b.

Figure 8a. Eliminating the Irrelevant Pixels Globally;

Figure 8b. Edge Region Irrelevant Pixels are Suppressed

4. Binocular Vision Ranging and SwingAangle Calculation

4.1. Binocular Vision Ranging Calculation Principle

Let the pixel coordinates be $S_L(x_L, y_L)$ and $S_R(x_R, y_R)$ on left and right images, respectively. Assuming the y coordinates are the same and we can calculate the 3D coordinates by disparity and trigonometry as follows:

$$\begin{cases} x_L = fx_c / Z_c \\ x_R = f(x_c - B) / Z_c \\ y = fy_c / y_c \\ Disparity = x_L - x_R \\ x_c = B \cdot x_L / Disparity \\ y_c = B \cdot y / Disparity \\ Z_c = B \cdot f / Disparity \end{cases} \tag{20}$$

Therefore, the pixel coordinates in camera coordinate system can be determined for any pixel on the left camera image as long as it can correctly match with the corresponding pixel on right image. We used parameters in section 3.2 to improve the matching method with matching primitives by gray level:

1) Building a convolution kernel window;

2) Covering left image by this window and selecting all pixels in this window;

3) Similarly, covering right image and select all the pixels;

4) Subtracting the left covered area from the right covered area and summing the absolute of them;

5) Moving the right window by step *3)* and *4)* repeatedly;

6) Finding the window which the correlation is weakest, that is, finding the best matched pixel block for left image.

4.2. The Swing Angle Calculation

We can get the disparity by stereo matching the left and right pixels, then calculate the 3D coordinates (x_w,y_w,Z_w) according to Eq. (20)-(21) and match the next pixel. Constructing 2 vectors with the maximum of Z coordinates $Z_{\max}$ and the minimum $Z_{\min}$ and recording the coordinates of corresponding pixels as $S_{\max}$=(x,y,$Z_{\max}$) and $S_{\min}$=(x',y',$Z_{\min}$). Calculating the swing angle by the vertical vector $\vec{S}_{\perp} = (0,0,-Z_{\max})$ and the vector with first pixel as vertexes simultaneously the final pixel as nadir $\vec{S}_{\angle} = (x'-x, y'-y, Z_{\min} - Z_{\max})$.

$$\theta = \arccos\left|\frac{\vec{S}_{\perp} \cdot \vec{S}_{\angle}}{\left|\vec{S}_{\perp}\right|\left|\vec{S}_{\angle}\right|}\right| = \arccos\frac{\left|Z_{\min} - Z_{\max}\right|}{\sqrt{(x'-x)^2 + (y'-y)^2 + (Z_{\min} - Z_{\max})^2}} \tag{21}$$

4.3. Analysis of the Experiment Results

Running this algorithm on OpenCV can get 6 angles as shown in Table 1.

Table 1. The Angle Measurement Results

iLabel	Z_w	Actual Value	Our Method	Relative Error
			Traditional Method	
1	Z_{max}(-220.65, 3429.76, 8716.13) Z_{min}(-227.24, 3432.32, 8665.55)	7°51′	**7°57′**	**1.3%**
			8°43′	11.1%
2	Z_{max}(122.65, 3428.45, 8720.03) Z_{min}(130.39, 3424.89, 8676.12)	11°04′	**10°58′**	**-0.9%**
			12°15′	10.6%
3	Z_{max}(-246.33, 3425.88, 8595.35) Z_{min}(-249.85, 3427.59, 8546.61)	4°32′	**4°35′**	**1.1%**
			4°12′	-7.3%
4	Z_{max}(145.52, 3426.22, 8601.74) Z_{min}(151.46, 3425.07, 8551.32)	6°54′	**6°50′**	**-1.0%**
			5°57′	-13.9%
5	Z_{max}(-240.78, 3427.61, 8472.81) Z_{min}(-248.11, 3430.45, 8423.36)	9°06′	**9°01′**	**-0.8%**
			10°06′	11.1%

6	Z_{max}(137.59, 3428.09, 8481.24) Z_{min}(149.98, 3426.67, 8433.43)	14°29′	**14°37′**	**0.9%**
			15°51′	9.5%

It can be seen that 3 swing angles data in the left part of image are slightly larger than actual values and the right data are generally smaller than actual value. Error of the former is slightly larger than that of the latter. This is probably because the left insulators are thin and blurry, while the right ones are rough clear. However, the accuracy of this method is higher than that of traditional method.

5. Conclusions

This paper analyzed the insulator shape characteristics and strength of symmetric at first, and then proposed an improved scanning algorithm with strength of symmetric as ROIs selecting parameter. In order to calculate the swing angle based on binocular vision, on the one hand we proposed double thresholds edge detecting algorithm and used statistical methods to analyze and remove irrelevant pixels to extract more accurate object, on the other hand calculated 3D coordinates of each pixel in every ROI and found out the highest and lowest pixels to establish 2 vectors, which is difficult to achieve a high precision for traditional method based on the ideal model. This method is almost not affected by sensor and topographic effects, makes a beneficial attempt for the image processing technology in the application field of swing angle calculation and it is helpful to feature extraction algorithm.

References

[1] L. XIAO, "A Thesis Submitted in Partial Fulfillment of the Requirements for the Degree of Master of Engineering", Wuhan, China: Huazhong University of Science and Technology, (in Chinese), **(2013)**, pp. 8.
[2] M. LI, Y. L. ZHANG and B. YANG, "Calculation and Analysis of Suspension Insulator Strings Windage Winimum Air Clearance", Electrical Measurement & Instrumentation, vol. 49, no. 555, **(2012)**, pp. 1
[3] X. B. HUANG, B. TAO and L.ZHAO, "Design of Transmission Lines New Wind Deviation On-line Monitoring System. High Voltage Engineering", vol. 37, no. 10, **(2011)**, pp. 2350-2355.
[4] S. E. WANG, G. WU and J. FAN, "Study on Flashover of Suspension Insulator String Caused by Windage Yaw in 500kV Transmission Lines", Power System Technology, **(2008),** vol. 32, no. 9, pp. 65-69.
[5] D. KONG, L. LI and X. LONG, "Finite Element Analysis of Dynamic Windage Angle of Suspended Insulator Strings", Electric Power Construction, vol. 29, no. 9, **(2008)**, pp. 5-9.
[6] H. LU, C. LIU and B. Xue, "Wind Deflection Angle Detection of Insulator Strings Based on IGHT", Water Resources and Power, vol. 31, no. 10, **(2013)**, pp. 185-188.
[7] R. Lienhart, "Video OCR: A Survey And Practitioner's Guide", Video Mining. Springer US, **(2003)**, pp. 155-183.
[8] P. Clark nd M. Mirmehdi, "Finding text regions using localized measures", In Proceedings of British Machine Vision Conference, **(2000)**, pp. 675-684.
[9] X. LIU, "Study on the segmentation of circle-like particle images", Changsha, China: Hunan University, **(2006)**, pp. 25.
[10] H Wang, X. U. Zhiwen and K. Xie, "Binocular Measuring System Based on OpenCV", Journal of Jilin University, vol. 32, no. 2, **(2014)**, pp. 188-194.
[11] S. Ayer and H. S Sawhney, "Layered representation of motion video using robust maximum-likelihood estimation of mixture models and MDL encoding, In: Int'l Conf. on Computer Vision, **(1995)**, pp. 777–784.

Authors

Rongbao Chen, received his B.Sc. degree in 1983 from Shanghai University, received his Ph.D. degree in 2010 from Shanghai University, now he is an associate professor in Hefei University of Technology. His main research interests include image recognition and application, modern sensor technologies, network communication technologies and intelligent control system. E-mail：crbwish@126.com

Yang Li, obtained his bachelor's degree of Hefei University of technology in 2013 and now is studying for his master's degree in Hefei University of Technology. The main research direction is image processing and application, modern sensor technology, intelligent control system. E-mail：lyhfut09@163.com